

# Reactive crystallization of basic magnesium carbonate

Hideki Tsuge\*, Yuji Takahashi and Eiji Fujiwara

Department of Applied Chemistry, Keio University  
3-14-1, Hiyoshi, Kohoku-ku, Yokohama, 223-8522 JAPAN  
TEL:81-45-563-1141 FAX:81-45-563-0446  
e-mail: [tsuge@applc.keio.ac.jp](mailto:tsuge@applc.keio.ac.jp)

To utilize magnesium in sea-water and to fix carbon dioxide from exhaust gasses, the direct carbonation method was used to precipitate basic magnesium carbonate, which is used as an anti-caking agent of NaCl by adhering to NaCl particle surface. It is necessary to make smaller particles to increase the surface area per unit mass of the particles. The aims of this study are to make clarify the mechanism of reactive crystallization of basic magnesium carbonate and to control its particle size.

## 1. INTRODUCTION

To utilize magnesium in sea-water and to fix carbon dioxide in exhaust gasses from power plants or factories, the direct carbonation method was used to precipitate magnesium carbonate, which is divided into basic magnesium carbonate and normal magnesium carbonate. As the following chemical formulas of basic magnesium carbonate are well known;  $4\text{MgCO}_3 \cdot \text{Mg}(\text{OH})_2 \cdot 8\text{H}_2\text{O}$  (Octahydrate),  $4\text{MgCO}_3 \cdot \text{Mg}(\text{OH})_2 \cdot 4\text{H}_2\text{O}$  (Hydromagnesite) and  $3\text{MgCO}_3 \cdot \text{Mg}(\text{OH})_2 \cdot 3\text{H}_2\text{O}$  (Artinite).

Tsuge et al.[1] presented the precipitation diagram of magnesium carbonate observed by direct carbonation method as a function of reaction temperature and initial concentration of magnesium hydroxide as shown in Figure 1. They observed  $4\text{MgCO}_3 \cdot \text{Mg}(\text{OH})_2 \cdot 8\text{H}_2\text{O}$  (hereafter abbreviated to BMC) and Magnesium Carbonate Trihydrate ( $\text{MgCO}_3 \cdot 3\text{H}_2\text{O}$ , MCT). Two types of morphologies of BMC were observed, that is, both spherical and tabular BMC particles were obtained for reaction temperature  $T \geq 60^\circ\text{C}$ . On the other hand, needlelike MCT particles were formed for  $T \leq 55^\circ\text{C}$ . In the figure shows coexistence of BMC and MCT. In the region B for  $55 < T < 60^\circ\text{C}$  the perfect petal BMC and needlelike MCT coexist, whereas in the region B' for lower  $\text{Mg}(\text{OH})_2$  initial concentration the coexistence of BMC and MCT particles was observed whose shapes were not perfect.

Basic magnesium carbonate is used as anti-caking agent of NaCl in Japan which acts by adhering to NaCl particle surface. To increase the surface area per unit mass of particle, it is necessary to make smaller basic magnesium carbonate particles.

The aims of this study are to make clarify the mechanism of reactive crystallization of BMC in direct carbonation method and to control the particle size of BMC for utilization as anti-caking agent of NaCl.

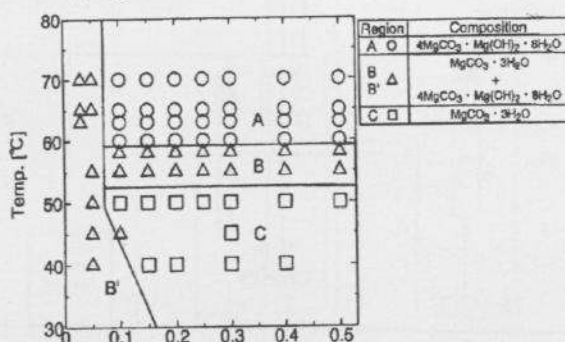


Figure 1. Precipitation diagram of magnesium carbonate

## 2. EXPERIMENTAL

First the magnesium hydroxide suspension was prepared in a 20 L stirred tank by the reactive crystallization through mixing 10L sodium hydroxide aqueous solution with 10L magnesium chloride aqueous solution. The by-product NaCl was removed using the following

procedures. After crystallization the  $\text{Mg}(\text{OH})_2$  suspension remained stationary for 2 days,  $\text{Mg}(\text{OH})_2$  particles settled and were separated by decantation and centrifugation. The condensed gel  $\text{Mg}(\text{OH})_2$  obtained was diluted with distilled water and prepared as 1.2 L  $\text{Mg}(\text{OH})_2$  aqueous solution for raw material of BMC.

Figure 2 shows the schematic diagram of the experimental apparatus for the reactive crystallization of BMC. The crystallizer used was a stirred tank reactor made of pyrex glass, considered to be a MSMR crystallizer. BMC particles were precipitated by blowing pure carbon dioxide gas into the suspension of magnesium hydroxide. The reaction was conducted at a constant temperature. The crystallization was completed when pH in the reactor became constant. The suspension solution in the reactor was sampled during and after the reaction. After the vacuum filtration and drying, the particles obtained were analyzed by the X-ray diffraction (XRD) and photographs by the scanning electron microscope (SEM) were taken. The diameter of particles was measured by a digitizer.

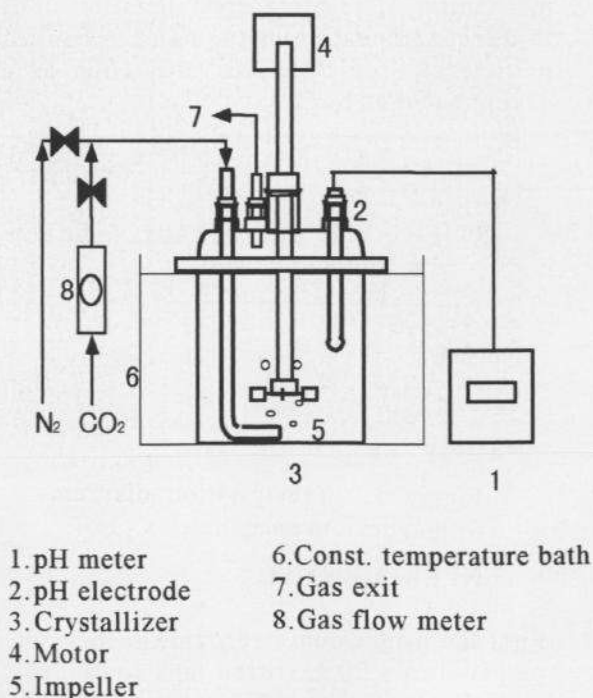


Figure 2. Schematic diagram of experimental apparatus

The experimental conditions were as follows;

- initial concentration of magnesium hydroxide : 0.20, 0.30 and 0.40 mol/L
- reaction temperature: 63, 70, 75 and 80 °C
- liquid volume in the reactor: 1.2 L
- stirrer speed: 600 rpm
- gas flow rate of  $\text{CO}_2$  : 480 mL/min

### 3. RESULTS AND DISCUSSION

#### 3.1 Precipitation mechanism of basic magnesium carbonate

In this study, the crystallization process of BMC particles was monitored by pH, SEM and XRD measurements. Figure 3 shows the time course of pH in the reaction solution under the conditions of 0.30 mol/L magnesium hydroxide suspended solution and reaction temperature 63 °C. The numbers in the figure correspond to the sampling points. Figures 4 (1)-(5) show the SEM photographs and XRD chart obtained at each sampling point.

At sampling point (1), as shown in Figure 4 (1), the pH decreased by the dissolution of  $\text{CO}_2$  gas in  $\text{Mg}(\text{OH})_2$  aqueous solution. The main part of particles was observed as  $\text{Mg}(\text{OH})_2$  from XRD and SEM photograph, whereas minute needlelike MCT crystals were also observed. In this stage BMC was not totally observed.

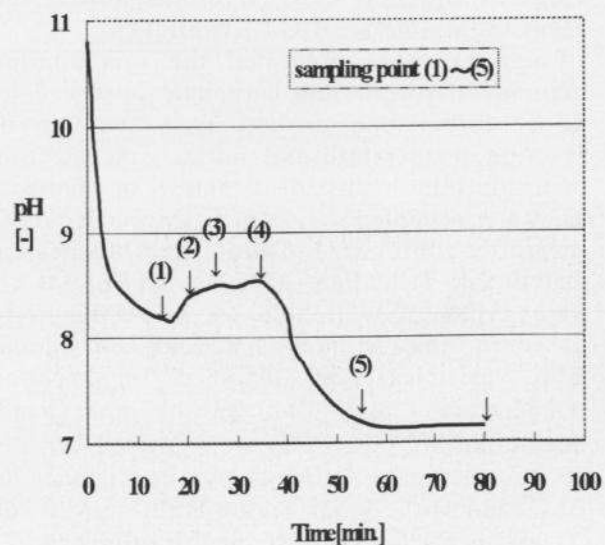
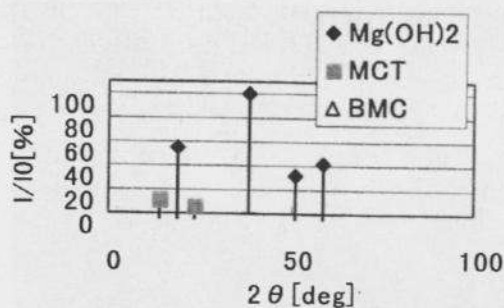
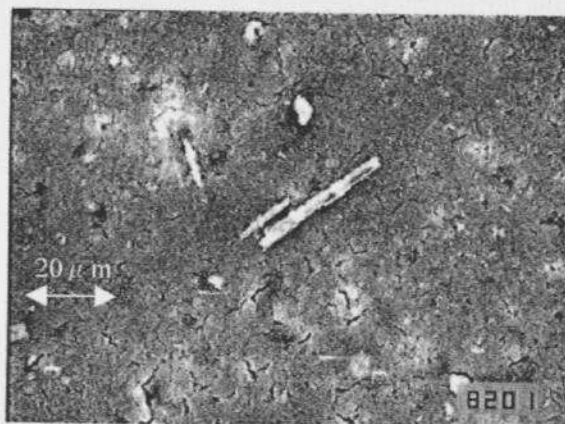


Figure 3. Time course of pH

At sampling point (2) as shown in Figures 4 (2-1) and (2-2), 2 types of particles were observed by increasing the supersaturation due to dissolution of  $\text{CO}_2$  gas. Firstly the spherical particles shown in Figure 4 (2-1) seem to be the precursor of BMC (mainly composed of  $\text{Mg}(\text{OH})_2$ ), while BMC was not observed by XRD. Secondly the needlelike MCT particles were formed as shown in Figure 4 (2-2) and the peaks of MCT were observed in XRD.



X-ray diffraction chart  
Figure 4 (1). Reaction time 15min

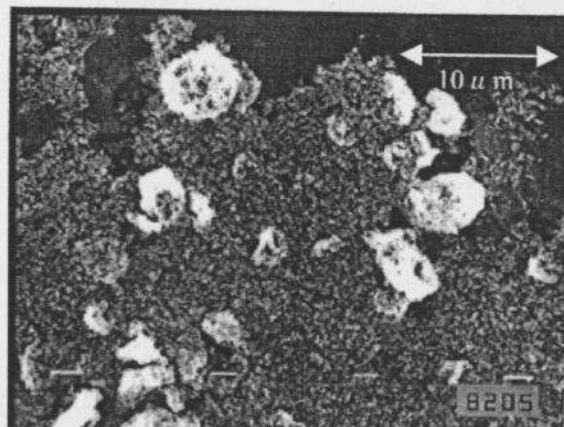


Figure 4 (2-1). Reaction time 20min

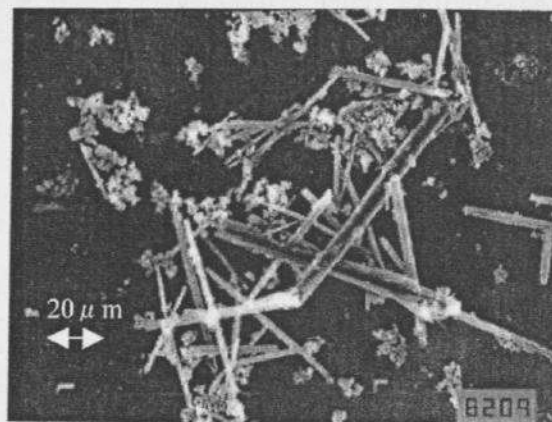


Figure 4 (2-2). Reaction time 20min

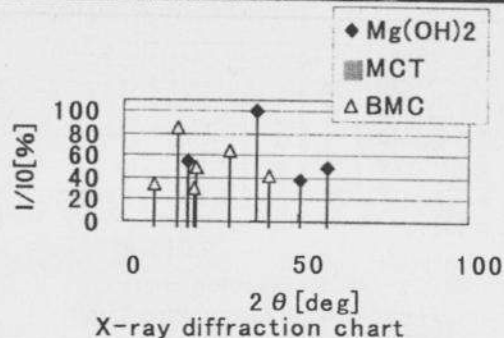
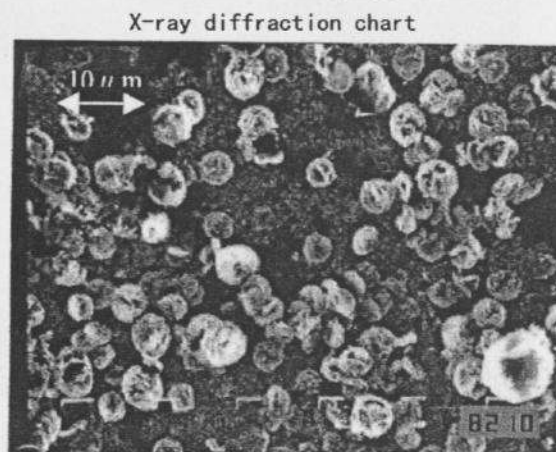
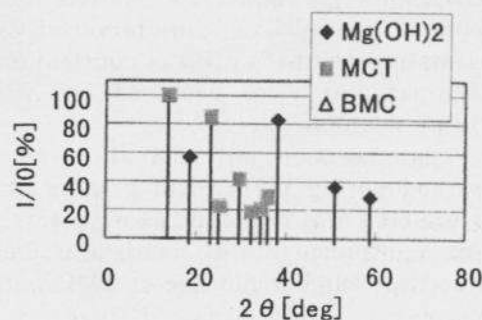


Figure 4 (3). Reaction time 25min



At sampling point (3) shown in Figure 4 (3), MCT was not found by dissolution at this temperature, but BMC and  $\text{Mg}(\text{OH})_2$  were observed by XRD. From the SEM photographs, the growth of spherical precursors in sampling point 2 was observed. The pH increased at sampling points (2) and (3) because the dissolved  $\text{CO}_2$  was consumed by the formation and growth of BMC.

At sampling point (4), shown in Figure 4 (4), the pH remained nearly constant, which was due to the immediate consumption of  $\text{CO}_2$  used for the growth of BMC particles. By XRD,  $\text{Mg}(\text{OH})_2$  was not observed but only BMC was observed. On SEM photographs petal BMC particles were observed. After that pH decreased again by the dissolution of  $\text{CO}_2$  and at sampling point (5) pH was constant and only BMC particles were observed by XRD and SEM photograph.

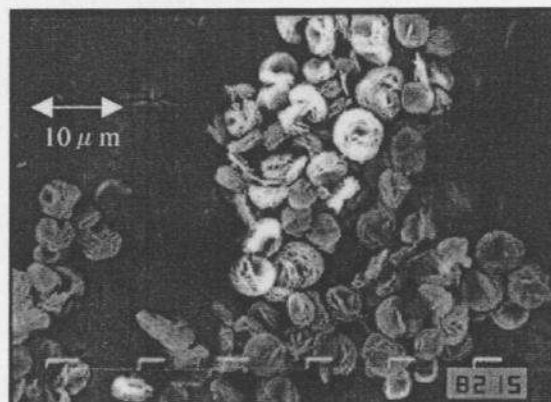
As agglomeration of particles was hardly observed during the growth process of BMC, the numbers of BMC particles were nearly same as those of precursors, so that it is assumed that the particle number and size of BMC were

controlled by the number of precursors particles. Mixtures of spherical and tabular BMC particles were obtained and their sizes were nearly same. From X-ray diffraction, it was proved that pure BMC particles were obtained.

As the pH increased on during the reaction at sampling points (1)-(3) as shown in Figure 3, be the dissolution of  $\text{CO}_2$  is considered to be the rate determining step. If the dissolution of  $\text{Mg}(\text{OH})_2$  were the rate determining step, pH would not increase because of the excess  $\text{CO}_2$  in the solution.

### 3.2. Effect of particle size of $\text{Mg}(\text{OH})_2$

The effect of particle size of  $\text{Mg}(\text{OH})_2$  on the precipitation process was examined in reactions 1 and 2. In the reaction 1,  $\text{Mg}(\text{OH})_2$  particles prepared by the described experiments were used, whereas in the reaction 2 we used the ground  $\text{Mg}(\text{OH})_2$  particles sold as a reagent. The particle size of  $\text{Mg}(\text{OH})_2$  in the reaction 2 was much larger than that in the reaction 1 as shown in Figure 5. By comparing the time course of pH shown in Figure 6, it is found that

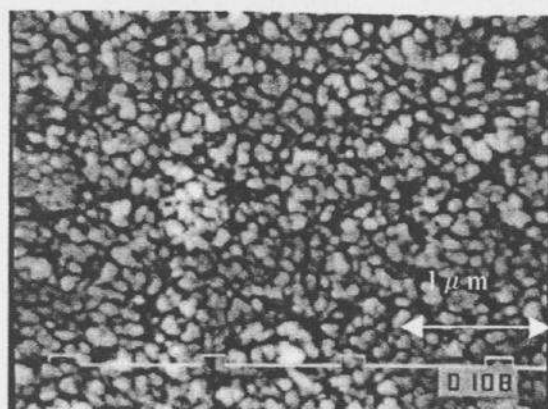
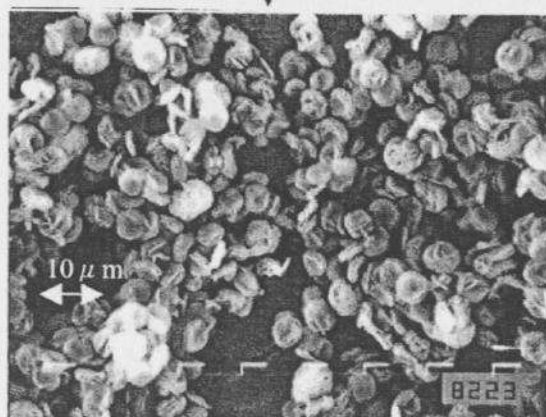


X-ray diffraction chart  
Figure 4 (4). Reaction time 35min



x-ray diffraction chart  
Figure 4 (5). Reaction time 55min

Reaction 1

Mg(OH)<sub>2</sub> particles

BMC particles

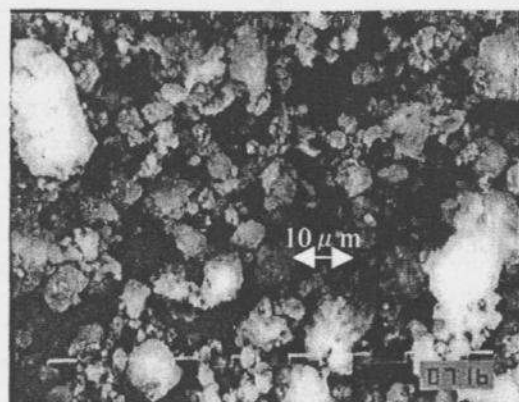
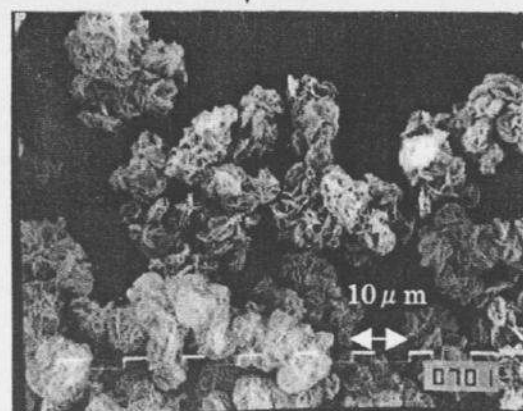
Figure 5 (1). SEM photographs

the pH increases due to the decrease of CO<sub>2</sub> concentration in the solution in the reaction 1, whereas the pH decreases gradually in the reaction 2. This leads to the conclusion that in the reaction 1 the dissolution of CO<sub>2</sub> was the rate determining step due to the small particle size of Mg(OH)<sub>2</sub>, on the other hand, in the reaction 2 as the particle size of Mg(OH)<sub>2</sub> was rather large and the surface area was so small that the dissolution of Mg(OH)<sub>2</sub> was the rate determining step.

### 3.3. Reaction time

Figure 7 shows the effects of the initial concentration Mg(OH)<sub>2</sub> and reaction temperature on the reaction time. The reaction time increased with increase in reaction temperature. Generally speaking, the reaction

Reaction 2

Mg(OH)<sub>2</sub> particles

BMC particles

Figure 5 (2). SEM photographs

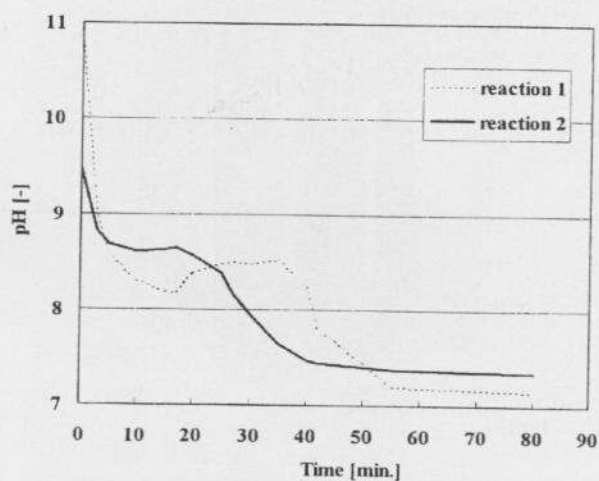


Figure 6. Time course of pH

rate increases and the reaction time decreases with increasing reaction temperature. On the other hand, the solubility of decreases with increase in temperature, which affects the relation between the reaction time and reaction temperature. This shows that the solubility of  $\text{CO}_2$  determines the reaction time.

### 3.4. Particle size of BMC

Figure 8 shows the effect of the initial concentration of  $\text{Mg}(\text{OH})_2$  and reaction temperature on particle size of BMC. The particle size of BMC increased with increase in  $\text{Mg}(\text{OH})_2$  initial concentration when the reaction temperature for reaction temperature was larger than  $70^\circ\text{C}$ . This was due to the fact that that  $\text{CO}_2$  concentration was lower than that of magnesium concentration so that the number of the precursor formed depended on only carbon dioxide gas concentration. As the feeding rate of  $\text{CO}_2$  was kept constant in spite of increase in  $\text{Mg}(\text{OH})_2$  initial concentration, the number of the precursor remained constant so that more magnesium hydroxide was consumed for the growth of precursor and the particle size of BMC increased. With an increase in reaction temperature, the solubility of BMC decreased and the precipitation rate of BMC increased so that the particle size increased. On the other hand, the particle size

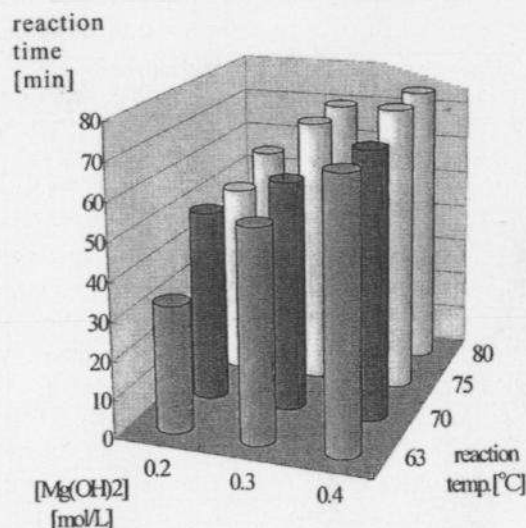


Figure 7. Effect of  $\text{Mg}(\text{OH})_2$  concentration and reaction temperature on reaction time

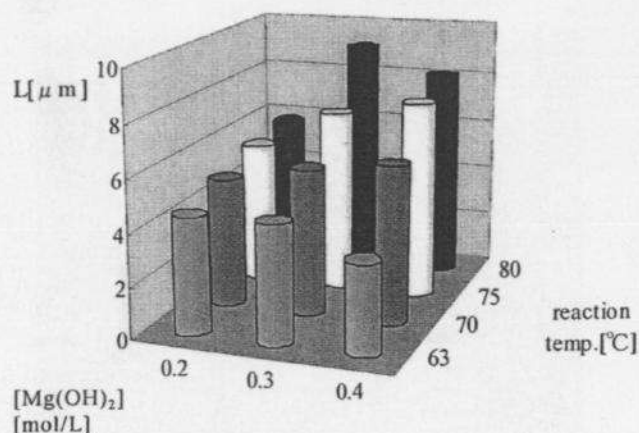


Figure 8. Effect of  $\text{Mg}(\text{OH})_2$  concentration and reaction temperature on particle size

increased with a decrease in initial concentration of magnesium for reaction temperatures  $\leq 63^\circ\text{C}$  due to the formation of MCT.

## 4. CONCLUSIONS

The precipitation process of BMC is composed of the formation of the precursor containing much  $\text{Mg}(\text{OH})_2$  and the growth of BMC. The particle size of BMC depended on the number of precursor as the agglomeration was not observed during growth of BMC.

The particle size of BMC was mainly influenced by the initial concentration of magnesium hydroxide and reaction temperature. By changing these two factors, it was possible to control the particle size of BMC between 4-9  $\mu\text{m}$ .

## REFERENCES

1. H. Tsuge, Y. Tanikawa and M. Sakakibara, Bull. Soc. Sea Water Sci., Japan, **50** (1996) 58.

## ACKNOWLEDGEMENT

The authors wish to thank Mr. Ninomiya, N. Kadigawa, K. and Shinohara T. from the Sea Water Science Research Laboratory in the Salt Industry Center of Japan for their valuable discussions.